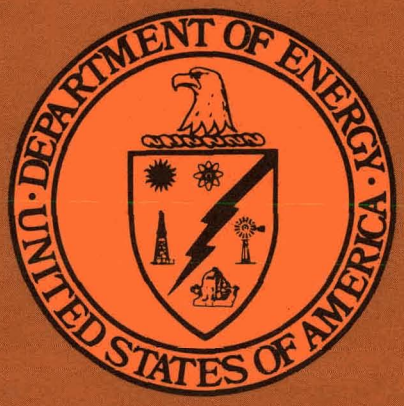

DOE/MC/19233-1472
(DE83017965)

SURFACE CHARACTERIZATION OF CONTAMINANT REACTANTS

For the Period June 14, 1982—June 14, 1983

By
Ranjani V. Siriwardane
Joseph V. Henry, Jr.

Work Performed Under Contract No. AT21-82MC19233

For
Morgantown Energy Technology Center
Morgantown, West Virginia

By
West Virginia University
Morgantown, West Virginia

TECHNICAL INFORMATION CENTER
UNITED STATES DEPARTMENT OF ENERGY

DISCLAIMER

DISCLAIMER

Available from the National Technical Information Service, U. S. Department of Commerce, Springfield, Virginia 22161.

Price: Printed Copy A03
Microfiche A01

Codes are used for pricing all publications. The code is determined by the number of pages in the publication. Information pertaining to the pricing codes can be found in the current issues of the following publications, which are generally available in most libraries: *Energy Research Abstracts (ERA); Government Reports Announcements* and Index (*GRA* and I); *Scientific and Technical Abstract Reports (STAR);* and publication NTIS-PR-360 available from NTIS at the above address.

DOE/MC/19233-1472
(DE83017965)
Distribution Category UC-90a

SURFACE CHARACTERIZATION OF CONTAMINANT REACTANTS

Covering the Period

June 14, 1982 to June 14, 1983

WVU Task Order No. 50

Contract No. AT21-82MC19233

for

Jason M. Cook
Exploratory Research Branch
Morgantown Energy Technology Center

Prepared by

Ranjani V. Siriwardane

Co-Principal Investigators

Joseph D. Henry, Jr.
Ranjani V. Siriwardane

Department of Chemical Engineering
West Virginia University
Morgantown, West Virginia 26506

ACKNOWLEDGMENT

The author would like to express appreciation to the Morgantown Energy Technology Center for both the use of its facilities and the support of this work under U.S. DOE Contract No. DE-AM21-79MC11284, Task Order No. 50. The author also likes to express her gratitude to Dr. J. M. Cook and Dr. K. H. Casleton without whose help and assistance this work would not have been possible.

TABLE OF CONTENTS

LIST OF TABLES

LIST OF FIGURES

ABSTRACT

Interactions of gaseous NO and SO_2 with Al_2O_3, SiO_2, and iron deposited on SiO_2 were carried out at temperatures 298, 473, and 673K. X-ray photoelectron spectroscopy (XPS) was used in the analysis. Pure Al_2O_3 and SiO_2 did not show any reaction with either NO or SO_2 at any of the three temperatures. Iron was deposited on SiO_2 in the metallic state. Both gases interacted with the Fe/SiO_2 system. Interaction increased with increasing iron deposition. Two forms of nitrogen were observed when NO was exposed to the Fe/SiO_2 system at 298K. They were identified as nitride and molecularly adsorbed NO. At 473K, the amount of nitride increased while molecularly adsorbed NO was not observed. Neither form of nitrogen was observed at 673K. Two forms of sulfur, sulfate and sulfide, were observed at 298K on the $SO_2/Fe/SiO_2$ system. At 473K, amount of sulfide increased while the amount of sulfate decreased. Neither form of sulfur was observed at 673K.

INTRODUCTION

Various gases like NO and SO_2 are produced during the coal combustion process. The removal of these corrosive gases from the combustion stream is very important. In order to understand the combustion stream, it is necessary to understand the reactions which occur between these pollutant gases and the constituents which would typically be found in ash, such as alumina, silica, and iron.

The purpose of this work was to investigate the interactions between gaseous NO and SO_2 with Al_2O_3, SiO_2, and iron deposited on a single crystal surface of SiO_2 using X-ray photoelectron spectroscopy (XPS). The exposure levels were on the order of several Langmuirs ($1L = 10^{-6}$ Torr-sec) for the single crystal samples, and the results are thought to be representative of the early stages of the reaction. Based on the results, reaction mechanisms have been deduced.

Various workers (1-6) have studied the adsorption of SO_2 on alumina and silica. Physisorption of SO_2 was found in most cases, and chemisorption of SO_2 was found on the γ-alumina (4,5). Interactions of NO with silica and alumina have also been investigated (7-14). Chemisorption of NO on silica was found only at 200 and 273K. Only physisorption was reported in the other systems.

However, none of the studies have dealt with the adsorption NO or SO_2 at low coverages in a flow system using XPS. The reactions have also not been investigated at elevated temperatures.

Only a few studies are reported on NO and SO_2 interaction with iron. None of the work is reported on the interaction of NO and SO_2 with iron deposited on silica. Blydholder and Cagle (17) demonstrated the formation of an SO_4 species on iron by infrared spectroscopy. The interaction of SO_2 with an iron film evaporated onto a sample probe was investigated by Furuyama, et. al (18), at 80 and 300K by XPS. The formation of sulfate and sulfide were observed. A photoelectron spectroscopic observation of iron surfaces exposed to NO at 200 torr and 1 atm was carried out by Honda and Hirokawa (19) at 273K. The formation of N, NO, NO_2, and NO_3 was observed on the surface. Infrared spectroscopic studies (20,21) indicated the formation of NO^+ on the iron surface. The interaction of NO at 5-20 Torr with iron evaporated onto stainless steel was studied by Kosaku and Ikeda (22). However, the reactions of NO on Fe or SO_2/Fe have not been carried out at elevated temperatures or at low pressures.

EXPERIMENTAL

The XPS spectra were recorded with a Vacuum Generators ESCA 3 spectrometer. This system consisted of separately pumped, liquid nitrogen trapped, spectrometer, and sample preparation chambers which routinely operated in the pressure range of 10^{-9}-10^{-10} Torr. The spectrometer was operated in the retarding mode with a pass energy of 50 eV and a slit width of 4 mm. The preparation chamber was equipped with a heated sample probe, an Ar ion etch gun for sample cleaning, and an evaporator for iron evaporation. The iron evaporator consists of a tungsten basket around which strips of thin iron foil is wrapped. Evaporations were carried out using resistive heating. Sample charging occurs on SiO_2 during XPS analysis because it is an insulator. Therefore, the charge correction on SiO_2 was done by assuming the binding energy of Si(2p) to be 103.7 eV. This value was established by taking C('s) peak to be 284.6 eV.

The Al_2O_3 and SiO_2 single crystals in these experiments were obtained from Atomergic Chemical Corporation. The Al_2O_3 single crystals were cut to produce a 1 mm x 10 mm x 10 mm sample with a (111) surface. The SiO_2 single crystals were cut to produce a 1 mm x 10 mm x 10 mm sample with a (001) surface. The samples were rinsed with acetone and were cleaned further by Ar etching. Carbon on the surface was negligible after 1/2-hour of Ar etching.

After cleaning the crystals, high purity NO or SO_2 (both supplied by Matheson) were transferred from a gas manifold to the preparation chamber using a Varian leak valve located on the preparation chamber. Gas exposures were carried out

at 298, 473, and 673K. During the exposures the gases flowed continuously over the sample.

RESULTS AND DISCUSSION

Section I: NO and SO_2 Exposures of Al_2O_3 and SiO_2

After exposing the SiO_2 surface to 50L of SO_2 at 298, 473, and 673K, no sulfur peak was detected in the binding energy region 164 eV to 194 eV. Thus, SO_2 did not chemisorb on SiO_2 at 298, 473, and 673K. This was in agreement with Galan and Smith (3) and Allen and Burevsk (4) in which it was found that the SO_2 is only physically adsorbed on SiO_2.

Similarly, sulfur peaks were not observed on Al_2O_3 when it was exposed to 50L of SO_2 at 298, 473, and 673K. This was contradictory to the observations made by Allen and Burevski (4) and Deo et al. (5), in which it was found that SO_2 was chemically adsorbed onto Al_2O_3.

When both Al_2O_3 and SiO_2 were exposed to 500L of NO, no nitrogen peak was detected in the binding energy region 388.0 to 418.0 eV at 298, 473, and 673K. Therefore, NO also did not chemisorb on SiO_2 and Al_2O_3. These results are in agreement with the results of Brown and Hall (7) in which they observed reversible adsorption of NO on alumina.

Section II: Deposition of Iron on Silica

The amount of iron deposition on silica was varied by changing the time of evaporation. The intensity of the iron peak was used as a measure of the amount of iron present on SiO_2 surface. Plot of intensity ratio of the iron

peak to silicon peak versus the evaporation time are shown in Figure 1. It is clear that the intensity of the iron peak increased with increasing evaporation time. The binding energies and the half width values of iron peak are listed in Table 1. The binding energies showed little variation during the evaporation times of 0 to 10 minutes. The half width of 3.4 eV indicated that only one form of iron was present on the SiO_2 system. In order to identify the form of iron present on SiO_2, the binding energies were compared with standard compounds. The binding energy of Fe(2p) peak on SiO_2 was closest to the value of the metallic form on an etched iron foil as shown in Table 1. The binding energy of iron on SiO_2 also compared well with the binding energy of metallic iron reported in the literature (23). Therefore, iron did not interact with SiO_2 and was deposited on the SiO_2 in the metallic form (Fe^{o}) for all of the evaporation times. The separation between Fe (2p 3/2) and Fe (2p 1/2) did not give a clear distinction between different Fe states as shown in Table 1.

Section III: Interaction of NO with Iron Deposited on Silica

Although NO did not react with pure silica when NO was introduced to the iron on the silica system at 298K, two forms of nitrogen were observed as shown in Figure 2. The major nitrogen peak appeared around 396.7 eV, while the second peak appeared around 400.6 eV. The Fe (2p 3/2) peak, both before and after the NO exposure, are shown in Figure 3. Before exposure to NO, the iron peak was narrow and had a half width equal to 3.5 eV, but after the exposure the half width increased to 6.7 eV. Since the broadening of the Fe peak occurred on the high binding energy side, it was possible that iron was oxidized to Fe^{+2} or Fe^{+3} state during the NO exposures. The oxygen peak of SiO_2 appeared around 532 eV. After the NO exposures, a second oxygen peak appeared around 530 eV.

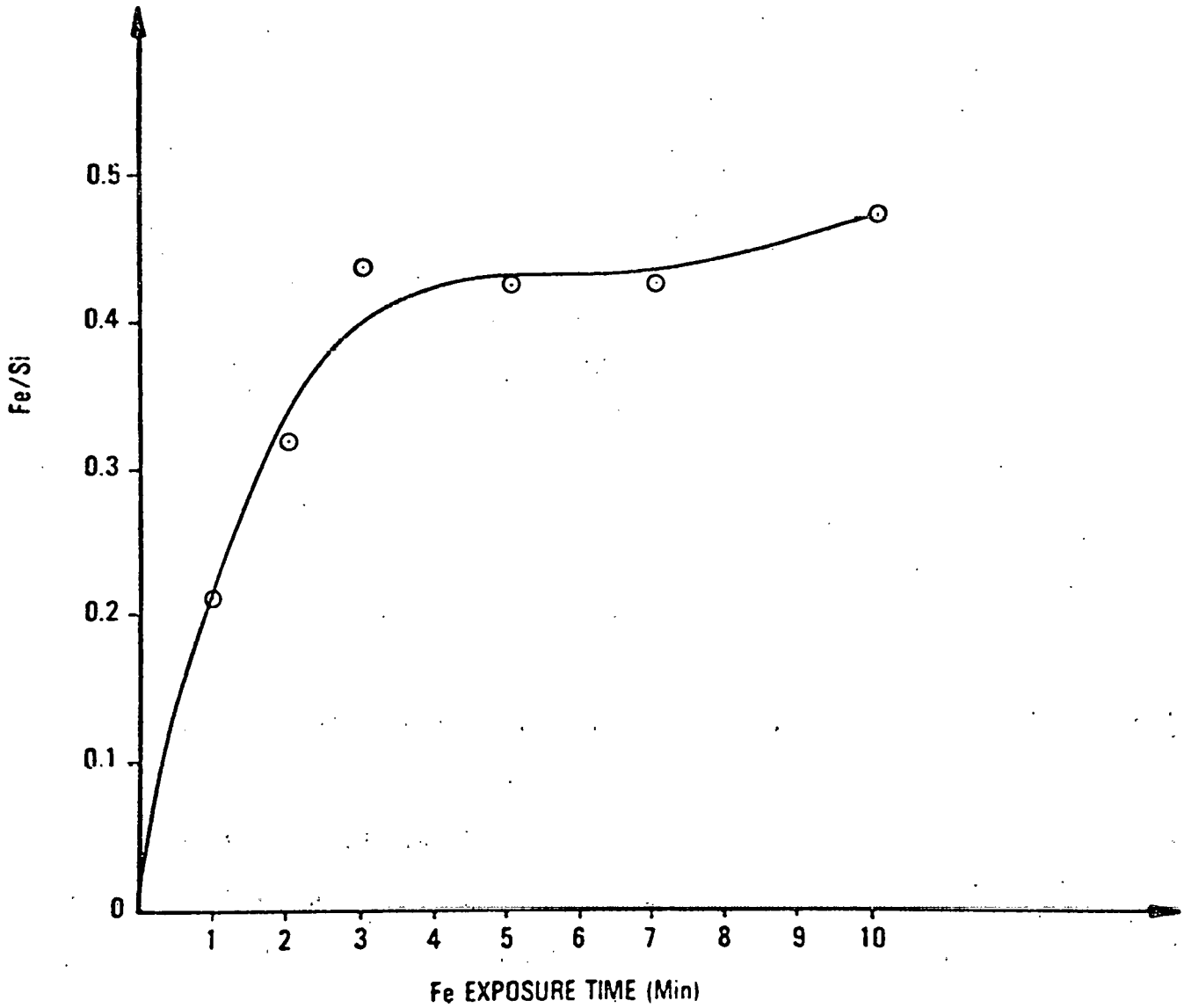

Figure 1

Fe/Si as a Function of Fe Exposure Time

TABLE 1

Binding Energies of Iron on SiO_2 as a Function of Exposure Time

Exposure Time (Minutes)	Binding Energy of Iron (eV)	Separation Between Fe 2P 3/2 and 2P 1/2	Width at Half Maximum (eV)
0	-	-	-
1	707.0	12.8	3.4
2	707.2	13.1	3.4
3	707.3	13.1	3.4
5	710.4	13.2	3.4
7	706.3	13.2	3.4
10	707.0	13.0	3.4
Standards			
$FeSO_4$	713.4	13.0	
Unetched Fe Foil	711.6	13.5	
Etched Fe Foil	708.5	13.3	
FeS	713.4	13.0	

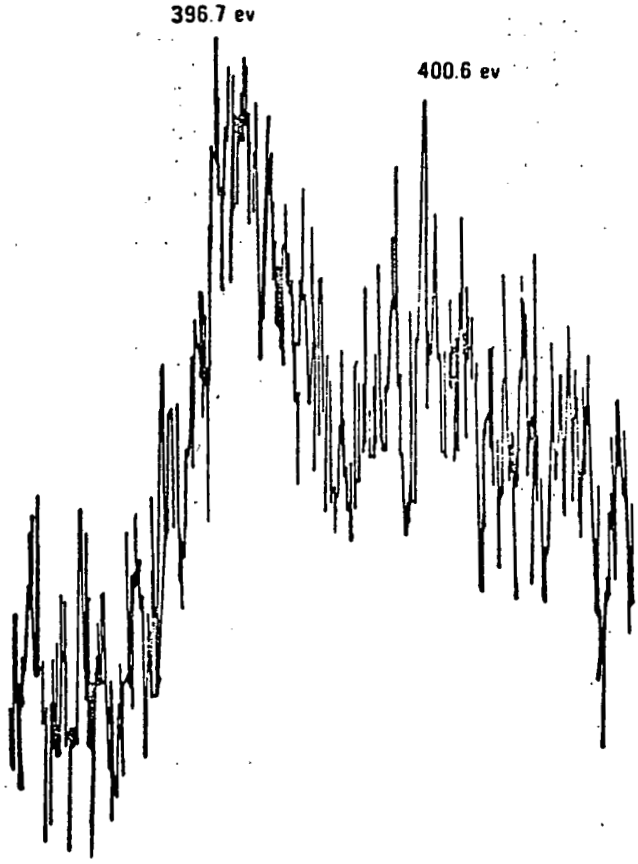

Figure 2

N(IS) Peaks for Reaction of NO with Fe/SiO_2

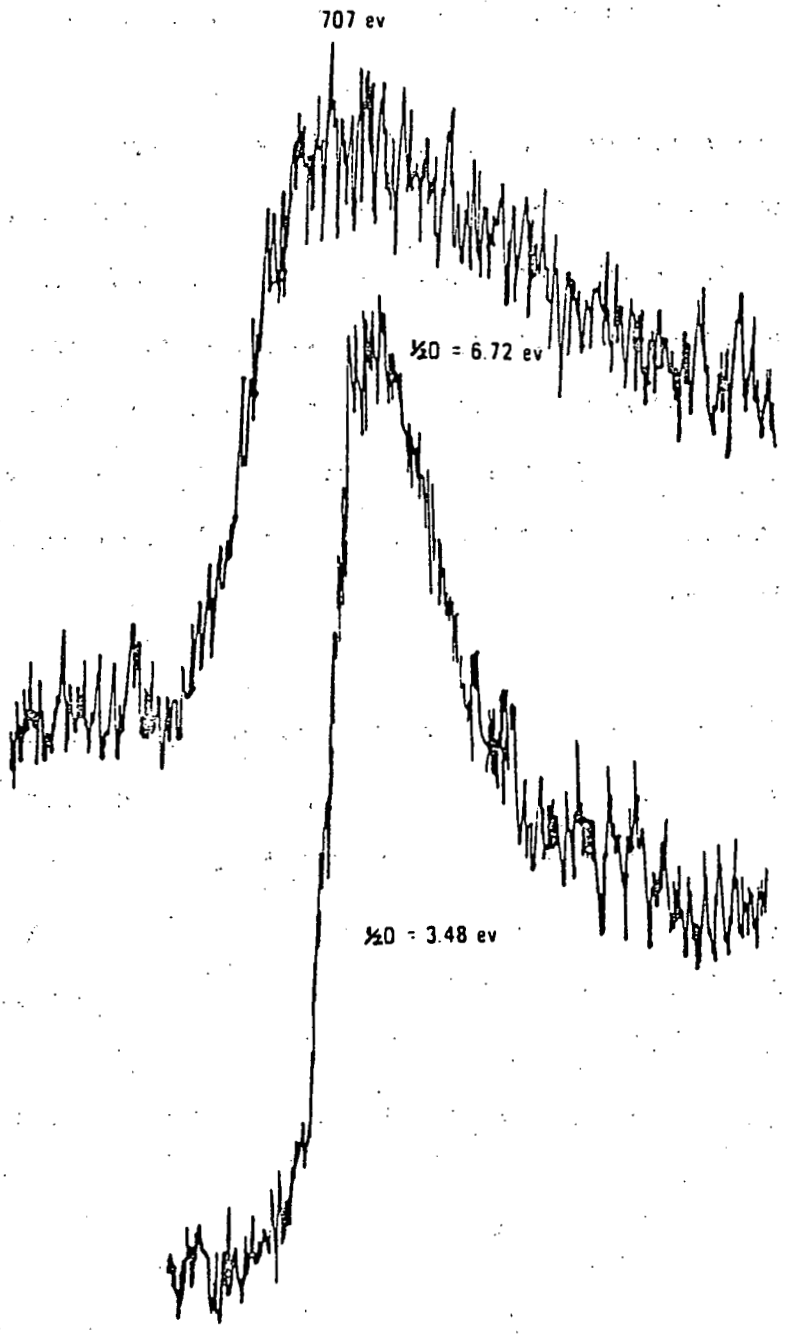

Figure 3

Fe(2P 3/2) Peaks as a Function of NO Exposures on SiO_2

The changes in the binding energies and intensities of iron and oxygen peaks as a function of NO exposures are further illustrated in Tables 2 and 3.

The intensities of the major nitrogen peak at 396.7 eV versus exposures are shown in Figure 4. The intensity reached a saturation value rapidly with increasing exposures. When the Fe/Si ratio was increased from 0.27 to 2.46, there was a significant increase in nitrogen intensity. However, the nitrogen intensity did not change when the Fe/Si ratio was increased to 00. Thus, deposition of iron on SiO_2 enhanced the adsorption of NO. The intensity of the second nitrogen peak at binding energy of 400.6 eV did not change with increasing Fe/Si ratio as shown in Figure 5.

When the reaction was carried out at 473K, only one form of nitrogen was observed at 396.7 eV. The plot of intensity of nitrogen versus exposure at 473K is shown in Figure 6. Similar to the results at 298K there was an increase in nitrogen intensity with increasing Fe/Si ratio. The nitrogen intensity was also higher at 473K than at 298K. When the reaction was carried out at 673K, no nitrogen peaks were observed in the binding energy range 388 eV to 418 eV. The binding energies of the nitrogen peaks at different exposures are listed in Table 4.

The plots of nitrogen intensity versus exposure at both 298 and 473K were similar to Langmuir adsorption isotherms (24). Therefore, the Langmuir equation, stated in equation [1], was used to calculate the nitrogen intensity (I_M) corresponding to a monolayer. The number of nitrogen atoms present at monolayer coverage (A_M^N) was calculated using equation [2]. The number of

TABLE 2

Binding Energies and Intensities of Iron Peak as a Function of NO Exposures on Fe/SiO_2

0L		1L		3L		5L		6L		72L	
BE(eV)	I	BE(eV)	I	BE(eV)	I	BE(eV)	I	BE(eV)	I	BE(eV)	I
T = 298K		Fe/Si = 0.27									
707.9	0.42	707.1	0.30	708.0	0.27	708.2	0.30	707.7	0.31	708.0	0.29
½d* = 3.8		½d = 5.3		½d = 5.3		½d = 5.3		½d = 5.4		½d = 6.2	
		Fe/Si = 2.46									
707.5	1.23	706.4	0.99	706.0	0.89	708.3	0.71	706.7	0.69	707.6	0.64
½d = 2.9		½d = 4.4		½d = 5.0		½d = 5.0		½d = 5.0		½d = 5.5	
		Fe/Si = ∞									
705.3	1.61	705.6	1.25	705.4	1.05	705.6	0.99	705.3	0.92	705.4	1.07
½d = 2.5		½d = 4.4		½d = 4.5		½d = 5.0		½d = 5.0		½d = 5.3	
T = 473K											
		Fe/Si = 0.38									
705.6	0.52	707.9	0.36	708.9	0.39	708.1	0.37	-	-	707.6	0.40
½d = 3.2		½d = 4.8		½d = 5.5		½d = 5.3				½d = 5.0	
		Fe/Si = 1.16									
706.6	0.83	707.3	0.59	707.0	0.48	707.5	0.52	-	-	707.5	0.54
½d = 3.2		½d = 5.0		½d = 5.0		½d = 5.0				½d = 5.2	
		Fe/Si = 2.19									
706.5	1.16	706.4	1.01	707.0	0.96	707.0	0.79	-	-	707.1	0.79
½d = 3.0		½d = 4.3		½d = 5.1		½d = 5.1				½d = 5.0	

* ½d = Width at half maximum.

TABLE 3

Binding Energies and Intensities of Oxygen Peak as a Function of NO Exposures on Fe/SiO_2

0L		1L		3L		5L		6L		72L	
BE(eV)	I	BE(eV)	I	BE(eV)	I	BE(eV)	I	BE(eV)	I	BE(eV)	I
T = 298K											
Fe/Si = 0.27											
532.6	2.66	532.5	2.28	532.5	2.51	532.5	3.00	532.4	2.76	532.2	2.73
Fe/Si = 2.46											
534.1	0.85	534.0	1.10	533.4	1.03	531.7	0.90	532.3	0.77	532.0	0.80
		531.6	1.07	530.5	1.30	529.1	1.07	529.2	1.20	529.2	1.27
Fe/Si = ∞											
531.9	0.34	531.7	0.34	531.3	0.39	531.7	0.46	531.1	0.49	531.2	0.53
		528.4	0.85	528.5	0.91	528.6	0.98	528.1	1.00	528.2	0.89
T = 473K											
Fe/Si = 0.38											
532.5	2.46	532.5	1.95	533.0	2.01	532.6	1.98	-	-	532.2	2.18
Fe/Si = 1.16											
532.2	1.5	532.7	1.20	532.2	1.20	532.1	1.32	-	-	532.0	1.36
		530.3	0.95	529.8	0.83	530.0	0.88	-	-	530.0	0.94
Fe/Si = 2.19											
532.5	0.85	531.7	0.89	531.7	0.99	532.4	0.86	-	-	531.6	0.88
529.1	0.39	529.2	1.02	529.7	1.32	529.6	1.23	-	-	529.7	1.24

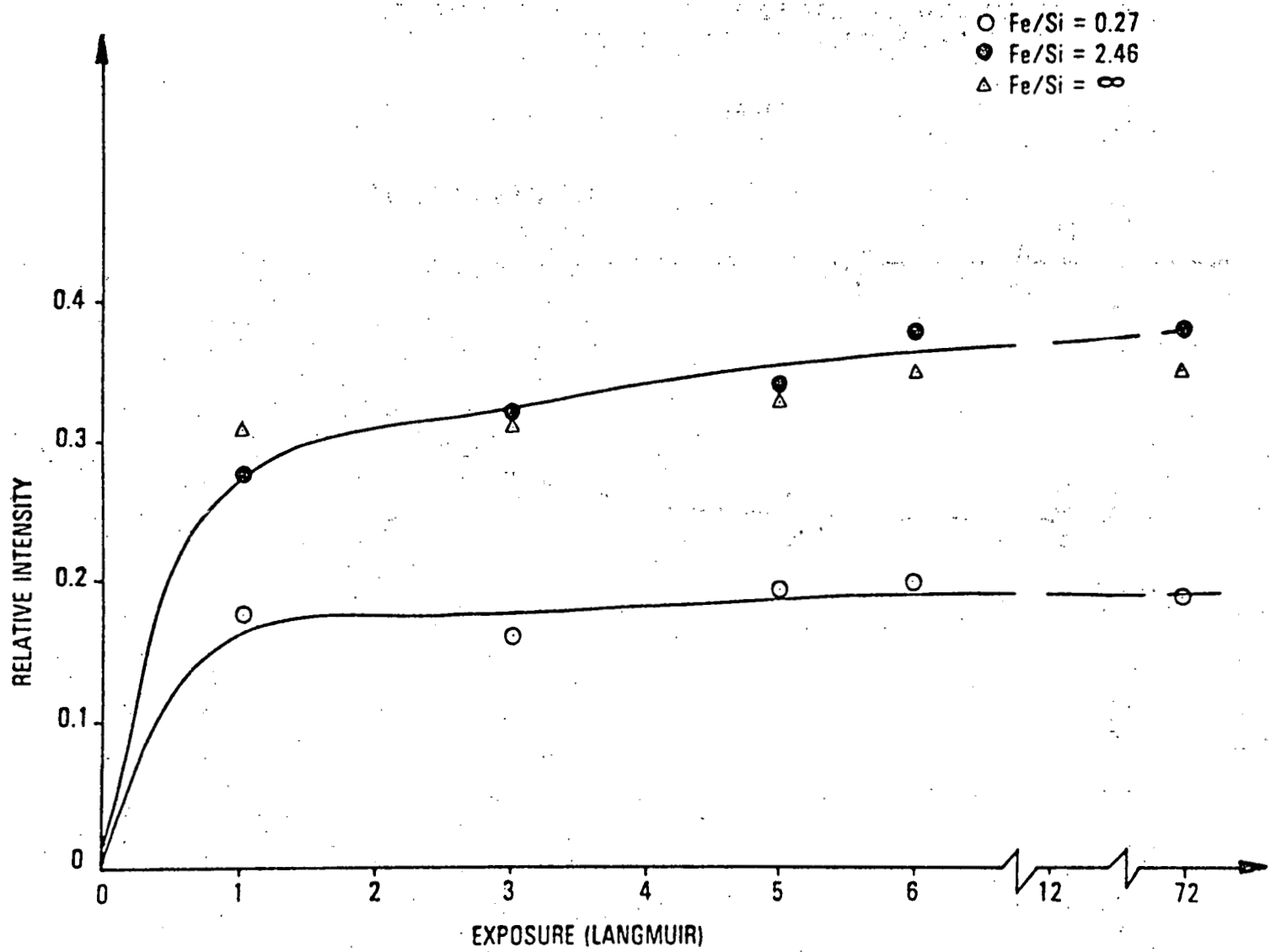

Figure 4

Intensity of N(IS)Peak at B.E. 396.7 eV as a Function of NO Exposures on Fe/SiO_2 at 298K (25°C)

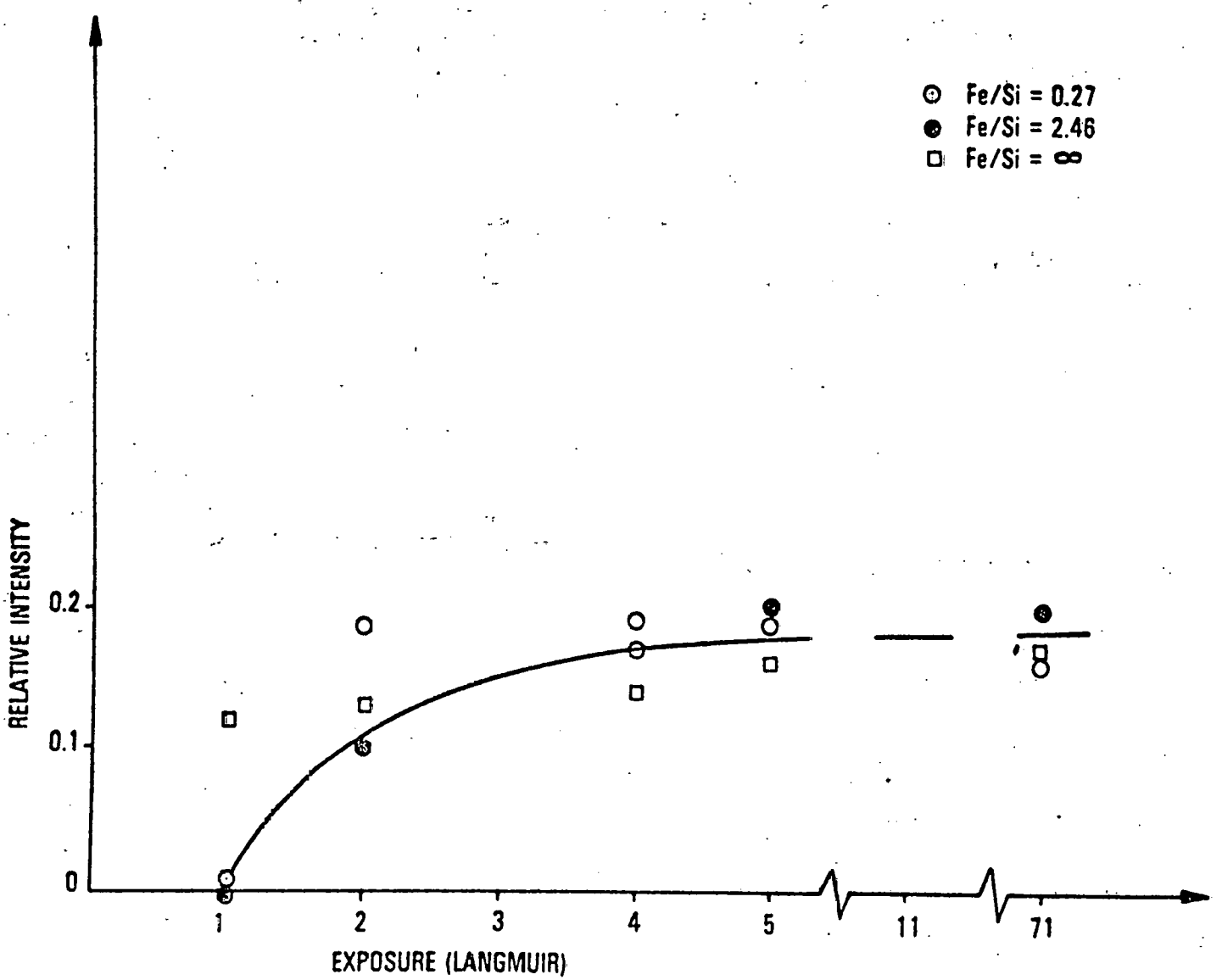

Figure 5

Intensity of N(IS) Peak at B.E. 400.6 eV as a Function of NO Exposures on Fe/SiO_2 at 298K (25°C)

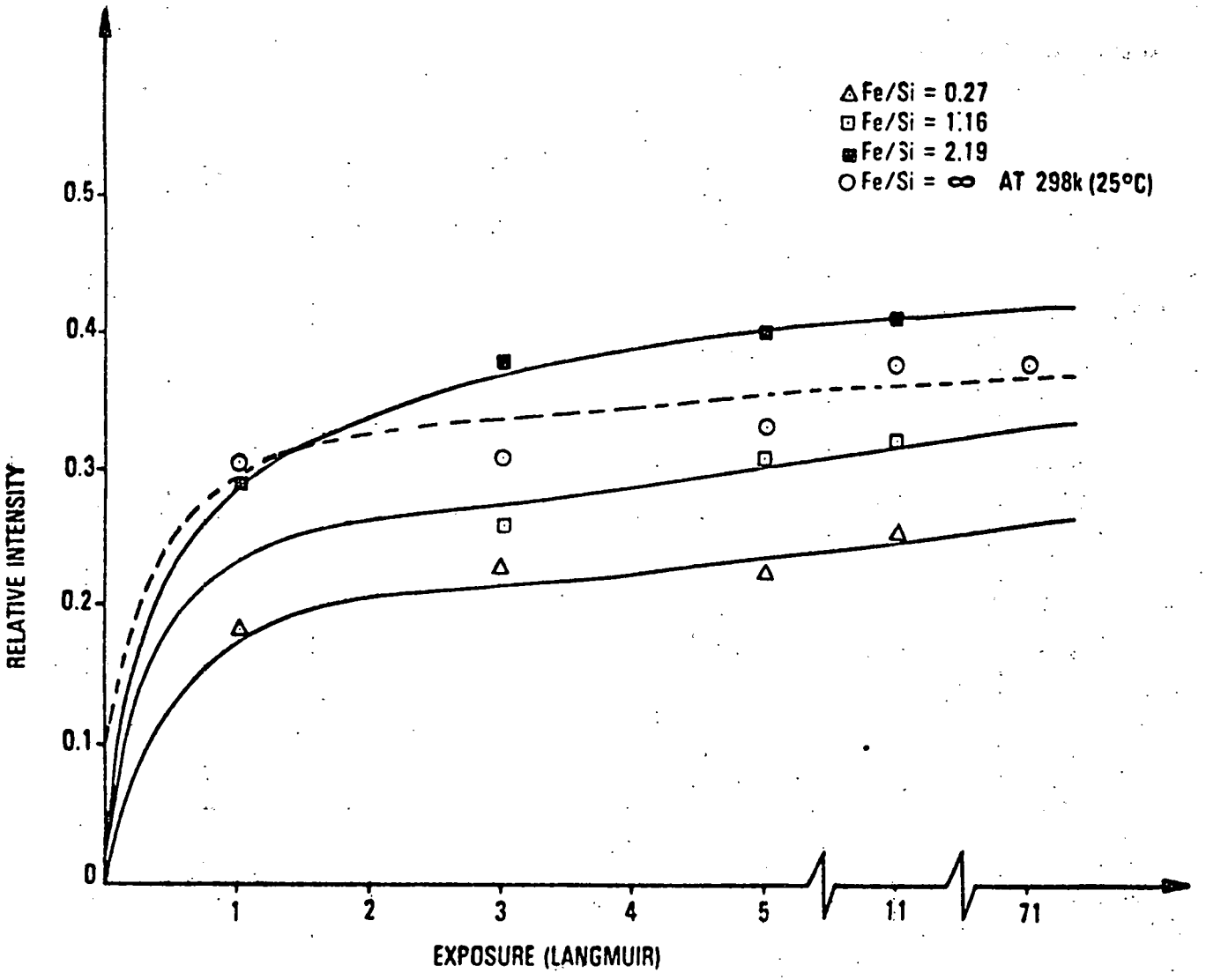

Figure 6

Intensity of N(IS) Peak at B.E. 396.7 eV as a Function of NO Exposures of Fe/SiO_2 at 473 K (200°C)

TABLE 4

Binding Energies of Nitrogen Peaks at Different Exposures on Fe/SiO_2

	1L	3L	5L	6L	72L
T = 298K					
Fe/Si = 0.27					
Si = 1.53	397.1	397.1 399.8	397.4 400.3	397.2 400.9	397.0 400.4
Fe/Si = 2.46					
Si = 0.50	396.1	397.7 401.0	396.7 400.7	396.7 400.6	396.6 400.1
Fe/Si = ∞					
	396.1 398.1	396.1 398.3	395.9 399.4	395.6 399.1	395.6 399.7
T = 473K					
Fe/Si = 0.38					
Si = 1.38	397.3	400.0	397.9	-	397.0
Fe/Si = 1.16					
Si = 0.71	397.0	396.8	397.2	-	397.2
Fe/Si = 2.19					
Si = 0.53	396.8	397.0	397.2	-	397.1

monolayers of iron (N^{Fe}) deposited on the SiO_2 system were calculated using equation [3]. The values of I_M, A^N_M, and N^{Fe} are listed in Table 5.

$$\frac{P}{I} = \frac{1}{bI_M} + \frac{P}{I_M} \qquad [1]$$

Where P = Exposure

b = Constant

I = Intensity of the N peak

$$A^N_M = \frac{\sigma_{Fe}\, \#_{Fe}}{\sigma_N} \cdot \frac{I_N}{I_{Fe}} \qquad [2]$$

where I_N = Intensity of nitrogen peak

I_{Fe} = Intensity of Fe peak

σ_N = Photoelectron cross section of N

σ_{Fe} = Photoelectron cross section of Fe

$\#_{Fe}$ = Number of iron atoms

$$N^{Fe} = \frac{\sigma_{Si}\, \lambda_{Si}\, N_o \cos\phi}{\sigma_{Fe}\, M_{Si}} \cdot \frac{I_{Fe}}{I_{Si}} \qquad [3]$$

TABLE 5

I_M, A_M^N and N^{Fe} Values for NO Exposures on Fe/SiO_2

$N^{Fe} \times 10^{15}$	I_M		$A_M^N \times 10^{15}$ No. of Atoms / cm^2	
	BE 396.7	BE 400.6	BE 396.7 eV	BE 400.6 eV
T = 298K				
0.30	0.19	0.16	0.10	0.08
0.66	0.38	0.20	0.14	0.08
1.08	0.35	0.16	0.21	0.09
T = 473K				
0.40	0.29	--	0.11	--
1.18	0.34	--	0.12	--
2.95	0.43	--	0.18	--

Where σ_{Si} = Photo electron cross section of Si

σ_{Fe} = Photo electron cross section of Fe

λ_{Si} = Mean free path of Si

N_0 = Avagadro Number

ϕ = 45°

I_{Fe} = Intensity of iron peak

I_{Si} = Intensity of Si peak at zero Fe coverage

M_{Si} = Molecular weight of Si

In order to identify the form of nitrogen present on the Fe/SiO_2 system, the binding energies were compared with standard compounds as shown in Table 6. The nitrogen peak at 396.7 eV compared well with the nitride binding energy. The second oxygen peak which appeared after the exposure of NO on the Fe/SiO_2 system also compared well with molecularly adsorbed oxygen. It was possible that NO dissociated on the Fe/SiO_2 system to form iron nitride. Similar dissociation of NO on other group VIII elements including, Platinum, Nickel, and Palladium was observed by previous workers (25-29). This dissociation reaction was enhanced by increasing iron on SiO_2 since there was an increase in nitrogen intensity with increasing iron deposition.

TABLE 6

Binding Energies of N(1S) Peak
for Standard Compounds

Compound	BE (eV)
$Fe_2(NO_3)_3$	407.1
Nitrates	407.0-408.0 (Brundle, 1976)
$Fe_4N + Fe_2N$	397.4
Nitride	396.5-398.5 (Brundle, 1976)
Pt -- NO (Molec)	401.0 (Bronzel, et al., 1976)
Ni -- NO (Molec)	399.9 (Bronzel, 1976)
Nitrosyl	400-403 (Brundle, 1976)
Nitrite	404-405 (Brundle, 1976)
$NO/Fe/SiO_2$	396.7
	400.6

When the reaction was carried out at 473K, there was an increase in the intensity of nitrogen at 396.7 eV. Thus, the dissociation reaction was enhanced by increasing the temperature to 473K. When the temperature was increased to 673K, no nitrogen was observed; however, adsorbed oxygen was still observed. It is possible that adsorbed nitrogen recombined to form N_2 and desorbed from the surface at 673K. Analysis of the desorbed products would be necessary to verify the reaction mechanism.

The second form of nitrogen observed at 298K compared well with the molecularly adsorbed NO. Since this form of nitrogen was not observed at 473 or 673K, it was possible that the molecularly adsorbed NO was desorbed from the surface at elevated temperatures.

Based on the XPS data, the reactions of NO with Fe/SiO_2 can be summarized as follows:

T = 298K

$$NO \xrightarrow{Fe/SiO_2} N_{ads} + O_{ads} \qquad [4]$$

$$NO \xrightarrow{Fe/SiO_2} NO_{ads} \qquad [5]$$

T = 473K

$$NO \xrightarrow{Fe/SiO_2} N_{ads} + O_{ads} \quad [6]$$

T = 673K

$$NO \xrightarrow{Fe/SiO_2} N_{ads} + O_{ads} \quad [7]$$

$$N_{ads} + N_{ads} \rightarrow N_2 \quad [8]$$

Section IV: Interaction of SO_2 With Iron Deposited on Silica

Although pure silica did not interact with SO_2 when the iron on silica system was exposed to SO_2 at 298K, two forms of sulfur were observed at 162.5 eV and 168.1 eV as shown in Figure 7. The major peak was at 168.1 eV. Broadening of the oxygen peak and the iron peak on the Fe/SiO_2 system was also observed after SO_2 exposure. The changes in the binding energies and the intensities of iron and oxygen are listed in Tables 7 and 8.

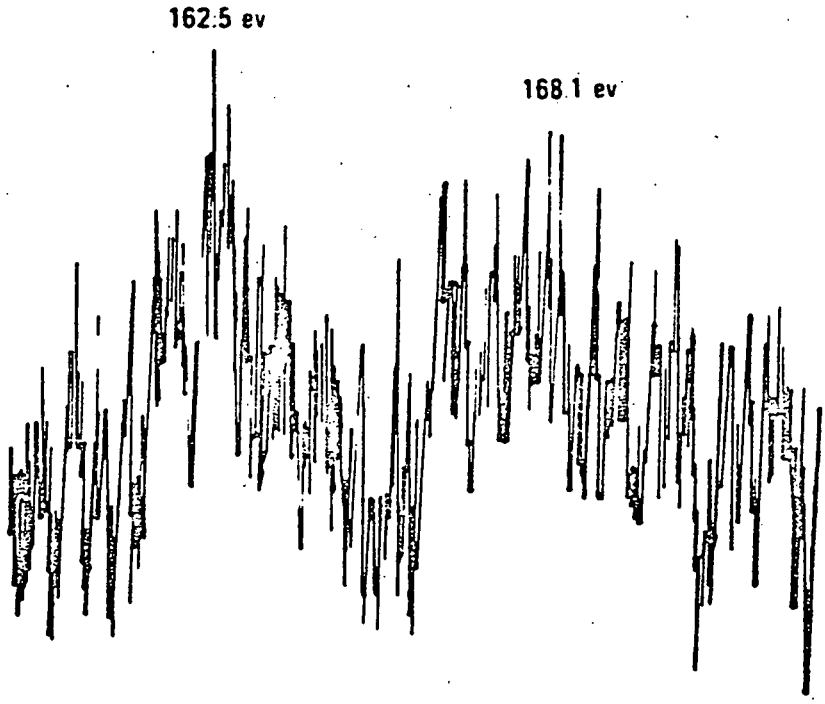

Figure 7

S(2P) Peaks for Reaction of SO_2 with Fe/SiO_2

TABLE 7

Binding Energies and Intensities of Iron Peak as a Function of SO_2 Exposures on Fe/SiO_2

	0L		1L		2L		4L		6L		12L	
	B.E.(eV)	I	B.E.(eV)	I	B.E.(eV)	I	B.E.(eV)	I	B.E.(eV)	I	B.E.(eV)	I
T = 298K												
Fe/Si = 1.56	706.3	1.28	707.0	0.97	706.4	0.62	707.0	1.0	707.1	0.8	707.5	0.91
Si = 0.82	½d* = 3.0		½d = 4.0		½d = 4.0		½d = 4.0		½d = 4.5		½d = 4.5	
Fe/Si = 196	705.7	1.06	706.2	1.16	707.2	0.92	707.3	1.05	-	-	707.3	1.08
Si = 0.43	½d = 3.0		½d = 4.0		½d = 4.0		½d = 4.0		-	-	½d = 4.0	
T = 473K												
Fe/Si = 1.58	706.8	1.15	706.8	0.89	706.6	0.84	706.6	1.02	-	-	706.7	0.85
Si = 0.73	½d = 3.0		½d = 3.1		½d = 4.0		½d = 4.0		-		½d = 4.0	
Fe/Si = ∞	706.8	1.25	706.3	1.35	706.5	1.26	706.3	1.30	-	-	706.4	1.34
	½d = 3.0		½d = 3.0		½d = 3.2		½d = 3.2		-		½d = 3.5	

* ½d = Width of half maximum.

TABLE 8

Binding Energies and Intensities of Oxygen Peak as a Function of SO_2 Exposures on Fe/SiO_2

	0L		1L		2L		4L		6L		12L	
	B.E.(eV)	I	B.E.(eV)	I	B.E.(eV)	I	B.E.(eV)	I	B.E.(eV)	I	B.E.(eV)	I
T = 298K												
Fe/Si = 1.56	531.8	1.06	531.9	1.43	530.7	1.27	530.7	1.57	531.8	1.34	532.3	1.62
Fe/Si = 1.96	531.4	0.82	531.0	1.23	531.5	1.09	530.7	1.02	-	-	530.6	1.09
					532.5	1.23	532.1	1.27	-	-	532.0	1.45
T = 473K												
Fe/Si = 1.58	532.3	0.96	532	0.96	532	1.06	532.3	1.42	-	-	532	1.19
Fe/Si = ∞	530.8	1.50	530.5	2.18	530	2.29	530.7	2.94	-	-	530.7	2.39

The intensity of the major sulfur peak, at a binding energy of 168.1 eV, versus exposure is shown in Figure 8. The intensity increased slightly with increasing iron deposition. When the temperature was increased to 473K, there was a significant decrease in the sulfur intensity, as shown in Figure 8.

The intensity of the sulfur peak at a binding energy of 162.5 eV versus exposure is shown in Figure 9. At 298K, there was no change in intensity of sulfur when the Fe/Si ratio was changed from 1.56 to 1.96. When the temperature was increased to 473K, there was an increase in sulfur intensity in contrast to the behavior of the sulfur peak at 168.1 eV as shown in Figure 8. Neither of the sulfur peaks was observed when the reaction was carried out at 673K.

The binding energies of the sulfur peaks at different exposures are listed in Table 9. The plots of the sulfur intensity versus exposure were similar to Langmuir adsorption isotherms (24). Therefore, the Langmuir equation stated in equation [1] was used to calculate the intensity (I_M) of sulfur at monolayer coverage. The number of sulfur atoms present at a monolayer coverage (A_M^S), and the number of monolayers of iron N^{Fe} deposited on SiO_2 were calculated using the procedure described in Section III. Values of I_M, A_M^S, and N^{Fe} are listed in Table 10.

In order to identify the form of sulfur present on the Fe/SiO_2 system, the binding energies were compared with the standard compounds shown in Table 11. The peak at 162.5 eV compared well with sulfide. Therefore, it was possible that SO_2 was dissociated into sulfur and oxygen on the Fe/SiO_2 system. Similar dissociation of SO_2 was reported by Furuyama, et al. (18), for iron deposited

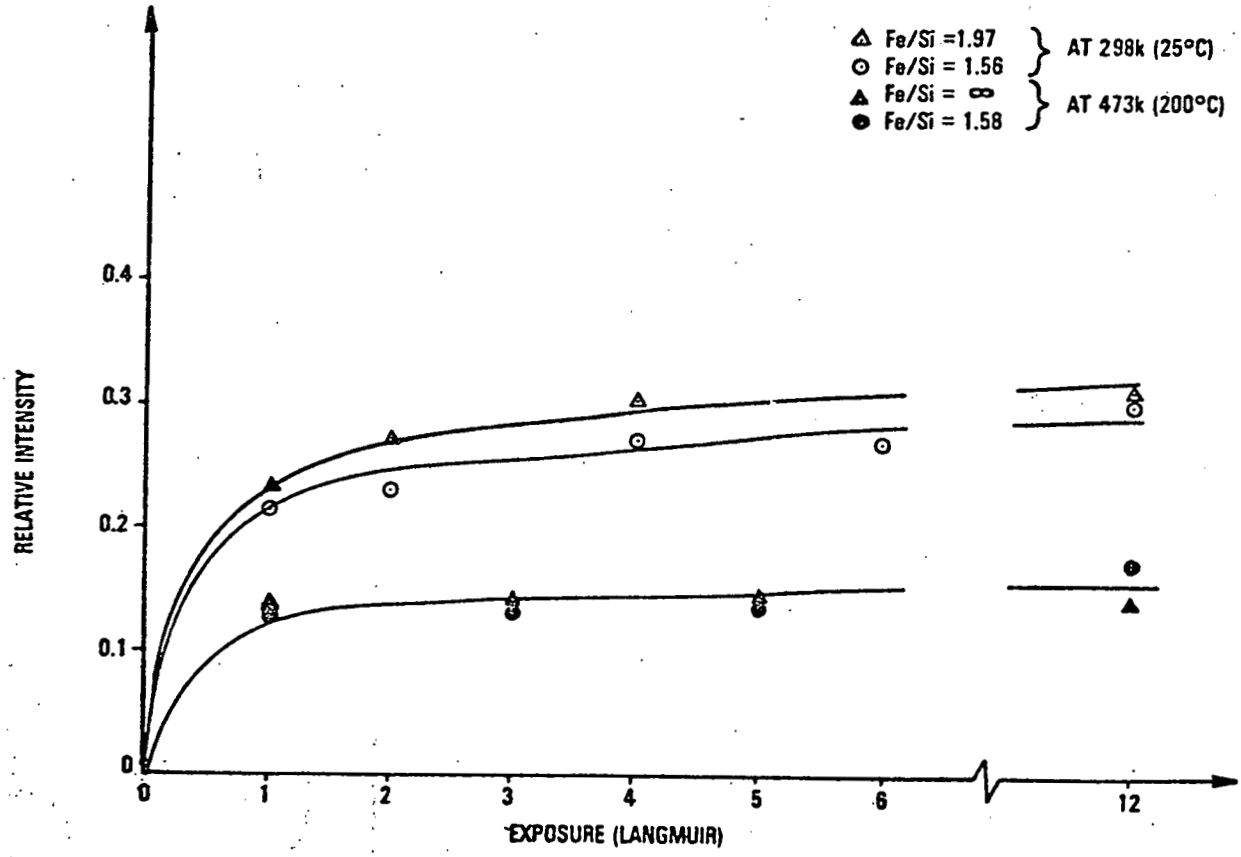

Figure 8

Intensity of S(2P) Peak at B.E. 168.1 eV
As a Function of SO_2 Exposures on Fe/SiO_2

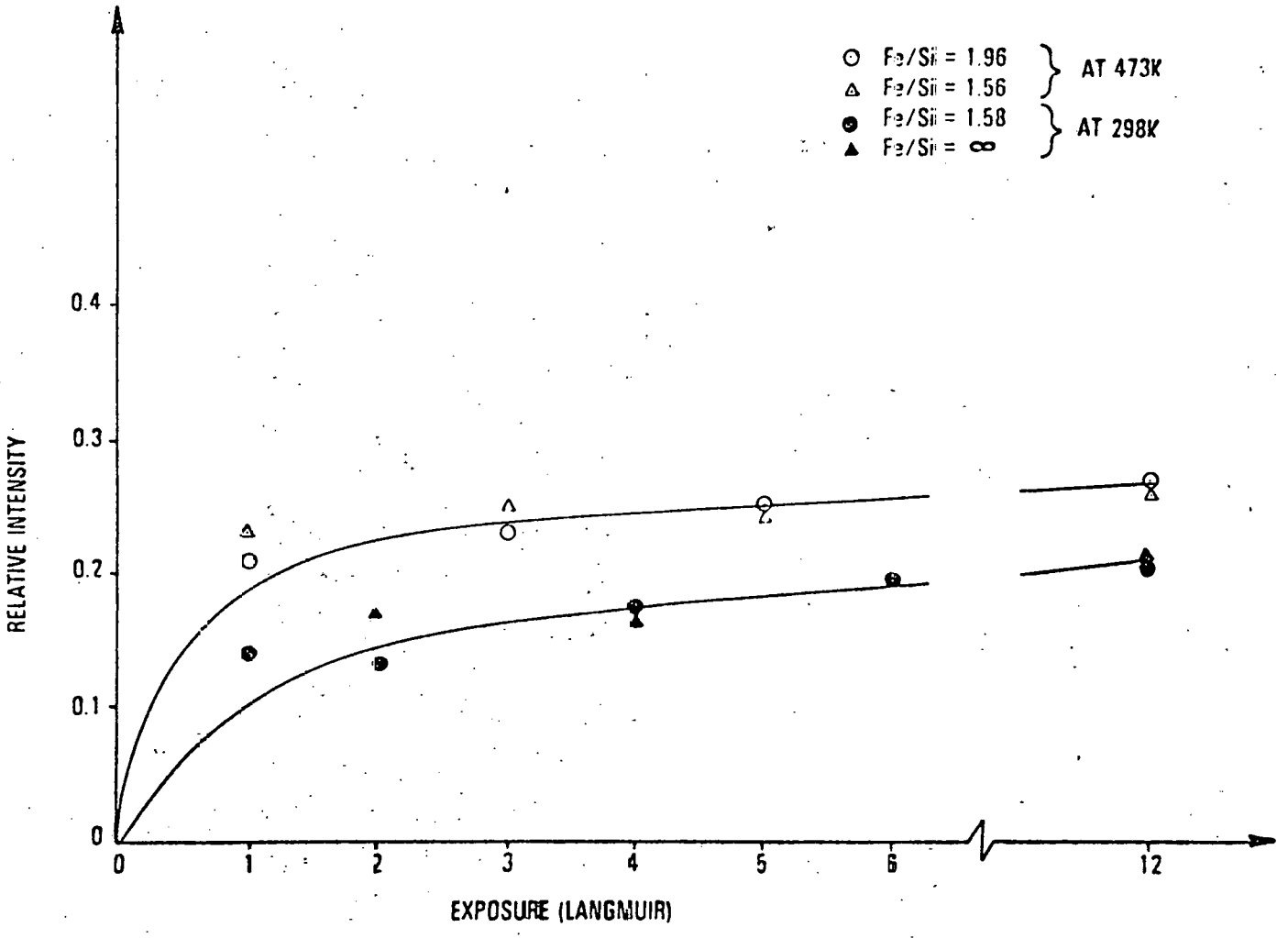

Figure 9

Intensity of S(2P) Peak at B.E. 162.5 eV as a Function of SO_2 Exposures on Fe/SiO_2

TABLE 9

Binding Energies (eV) of Sulfur Peak as a Function of SO_2 Exposures on Fe/SiO_2

	1L	2L	4L	6L	12L
T = 298K					
Fe/Si = 1.56	167.4	169.7	167.7	167.9	167.6
	162.5	163.7	161.6	162.4	162.5
Fe/Si = 1.96	168.5	167.9	169.6	-	167.3
		161.8	162.1	-	162.0
T = 473K					
Fe/Si = 1.58	167.0	166.5	167.0	-	167.0
	161.7	161.8	162.3	-	161.5
Fe/Si = ∞	167.0	167.5	167.0	-	167.0
	161.4	162.0	161.7	-	161.8

TABLE 10

I_M, A_M^S, and N^{Fe} Values for SO_2 on Fe/SiO_2 System

	I_M		$A_M^S \times 10^{15}$	No. of Atoms / cm^2
$NFe \times 10^{15}$	BE 168.1 eV	BE 162.5 eV	BE 168.1 eV	BE 162.5 eV
T = 298K				
0.39	0.33	0.21	0.12	0.08
0.47	0.32	0.22	0.12	0.08
T = 473K				
0.42	0.14	0.24	0.05	0.09
0.46	0.18	0.27	0.07	0.10

TABLE 11

Binding Energies of S(2P) Peak
of Standard Compounds

Compound	S(2P) (ev)
$CaSO_4$	169.9
$CaSO_3$	168.9
$FeSO_4$	168.6
FeS	161.0
$Fe_2(SO_4)_3$	168.4
SO_2/AU at 80K	167.4 (Furuyama et al., 1978)
$SO_2/Fe/SiO_2$	162.5
	168.1

on a tungsten filament. Since the intensity of this sulfur peak increased when the temperature was increased to 473K, there is more dissociation of SO_2 at 473K on the Fe/SiO_2 system. When temperature was increased to 673K, the sulfur peak at 162.5 eV was not observed. It was possible that the adsorbed sulfide was desorbed at 673K.

The other form of sulfur, observed at a binding energy of 168.1 eV, compared well with sulfate. However, a clear distinction between SO_2, SO_3, and SO_4 cannot be made based on binding energy. The iron sulfite form is not a very stable compound. Therefore adsorbed sulfur is more likely to be sulfate. Sulfate formation on iron was previously observed by Furuyama, et al. (18). Stinespring and Cook (30) observed sulfate formation when SO_2 was introduced on CaO. This sulfate form of sulfur decreased at 473K and was completely removed from the surface at 673K.

The reactions of SO_2 on the Fe/SiO_2 system based on XPS data can be summarized as follows:

T = 298K

$$SO_2 \xrightarrow{Fe/SiO_2} S_{ads} + O_{ads} \qquad [9]$$

$$SO_2 + 2O_{ads} \xrightarrow{Fe/SiO_2} SO_4 \qquad [10]$$

At 473K, reaction [9] increased while the reaction [10] decreased. The two adsorbed products, sulfide and sulfate, were completely desorbed at 673K.

REFERENCES

1. Khulbe, K. C., and Mann, R. S., J. Catal. 51, 364-71 (1978).

2. Glass, R. W., and Ross, R. A., Can. J. Chem. 49 2832-39 (1971).

3. Galan, M. A., and Smith, J. M., J. Catal. 38, 206-13 (1975).

4. Allen, T., and Burevski, D., Powder Technol. 21, 91-96 (1978).

5. Deo, A. V., Dalla Lana, J. G., and Habgood, H. W., J. Catal. 21, 270-81 (1971).

6. Jones, W. J., and Ross, R. A., J. Chem. Soc. 4 Part II, 1021-6 (1967).

7. Brown, C. E., and Hall, P. G., J. of Colloid Interface Sci. 42(2), 334-341 (1973).

8. Smith, R. N., Lesnini, D., and Mooi, J., J. Phys. Chem. 60, 1063-1066 (1956).

9. Douglas, T. B., "The Physical and Chemical Adsorption of Nitric-Oxide on Alumina and Other Oxides," Ph.D. Dissertation, Stanford University (1975).

10. Iwaizumi, M., Kubola, S., and Isobe, T., Bull. Chem. Soc. of Japan 47, 597-599 (1974).

11. Solbakken, A., and Reyerson, L., J. Phys. Chem. 68, 1622 (1959).

12. Huang, N. L., and Van Vleck, J. H., J. Chem. Phys. 50, 2932-2935 (1969).

13. Lunsford, J., J. of Catal. 14, 379-385 (1969).

14. Lunsford, J., Zingery, L., and Rosynek, M., J. of Catal. 38, 179-188 (1975).

15. Pozdnyakov, D., and Filimonor, V., Advances in Molecular Relaxation Processes 5, 55-63 (1973).

16. Brown, C., and Hall, P., Surface Sci. 36, 569-579 (1973).

17. Blyholder, G. D., and Cagle, G. W., Environ. Sci. Technol. 5, 158 (1971).

18. Furuyama, M., Kishi, K., and Ikeda, S., J. of Electron Spec. and Related Phenomena 13, 59-67 (1978).

19. Honda, F., and Hirokawa, K., J. of Electron Spec. and Related Phenomena 8, 199-211 (1976).

20. Blyholder, G., and Allen, M. C., J. Phys. Chem. 65, 3998 (1965).

21. Terenin, A., and Rocu, L. M., Spectrochim. Acta. 13, 946 (1959).

22. Kishi, K., and Ikeda, S., Bull. of the Chem. Soc. of Japan 47(10), 2532-2536 (1974).

23. Wagner, C. D., Riggs, W. M., Davis, L. E., Moulder, J. F., and Muilenberg, G. E., Handbook of X-Ray Photoelectron Sepctroscopy, Perkin-Elmer Corporation, 1979.

24. Adamson, A. W., "Physical Chemistry of Surfaces," Third Edition, John Wiley Sons, 1976.

25. Comrie, C. M., Weinberg, W. H., and Lambert, R. M., Surface Sci. 57, 619-631 (1976).

26. Bomel, H. P., and Pirug, G., Surface Sci. 62, 45-60 (1977).

27. Price, G. L., Sexton, B. A., and Baker, B. G., Surface Sci. 60, 506-526 (1976).

28. Brundle, C. R., J. Vac. Sci. Technol. 13(1), 301 (1976).

29. Conrad, H., Ertl, G., Kuppers, J., and Latta, E. E., Surface Sci. 50, 296-310 (1975).

30. Stinespring, C. D., and Cook, J. M., J. of Elec. Spec. and Related Phenom. (accepted for publication).

☆ U.S. GOVERNMENT PRINTING OFFICE: 1983—746-081/2172